



Work function tuning of an ultrathin MgO film on an Ag substrate by generating oxygen impurities at the interface

Sung Beom Cho, Kyung-Han Yun, Dong Su Yoo, Kiyong Ahn, Yong-Chae Chung *

Hanyang University, 222 Wangsimni-ro, Seongdong-gu, Seoul 133-791, Republic of Korea



ARTICLE INFO

Available online 4 January 2013

Keywords:
MgO/Ag
Work function
Interface defect
Oxygen impurity

ABSTRACT

Density functional theory was used to investigate the electrostatic effect of various oxygen impurities at the interface of MgO/Ag, including interstitial oxygen defects, substitutional oxygen defects, and reconstructed substitutional oxygen defects. When interstitial and reconstructed substitutional oxygen impurities were generated at the interface, an additional bond with the film was formed and the work function of the interface increased. On the other hand, in the case of substitutional oxygen generated at the interface, the oxygen impurities migrated into the Ag subinterface layer and the work function of the interface was slightly decreased. It can be inferred that the origin of the work function change is the dipole moment induced by oxygen impurities. The results of this study indicate that the work function of MgO/Ag (001) can be finely tuned with interfacial oxygen impurities.

© 2012 Elsevier B.V. All rights reserved.

1. Introduction

Ultrathin oxide films on metallic substrates have received considerable attention for application in the field of catalyst [1,2]. In particular, MgO thin films epitaxially grown on Ag are one of the most commonly studied catalytic substrates due to its simple structure and slight lattice mismatch [3]. The MgO/Ag combination permits the chemical reactions such as N₂O reduction [4], water dissociation [5], and charging of adsorbates [6] which are not observed on the corresponding single crystal surface. It is believed that such chemical activations are triggered by charge transfer from the interface to adsorbate in experimental [7,8] and theoretical analyses [9]. The charge transfer is explained by a reduced work function of the metal induced by the “compression effect” [10]. The compression effect occurs when the dielectric layer pushes partially spread electrons out of the surface back into the metal layer, thus changing the surface dipole and lowering the metal work function. The modified work function increases the tunneling properties from the interface to the adsorbate. Therefore, the value of the work function is one of the key parameters in determining the charging behavior of the adsorbates and direct measuring of the work function has been intensively studied [11,12].

Recently, Jung et al. reported enhanced chemical reactivity by artificially manipulating the oxide/metal interface structure [13]. Such manipulated interface structure can be generated from the deposition process. Before film deposition, surface vacancies [14], rippling [15], and dislocation [16,17] can be generated through the presputtering process onto single crystal Ag. Also, adsorbed oxygen can occupy hollow site and

vacancy sites of the Ag surface in the oxygen rich atmosphere [18]. Moreover, such point defects on metallic substrates can be artificially generated by directly picking up single Ag, Mg, or O atoms with atomic force microscopy tips [19]. Through such a process, the interstitial and substitutional oxygen impurities can be generated at the interface.

Even though buried oxygen defects are suggested in other studies, their electronic structure and induced electrostatic effects are not fully understood due to its practical difficulty of direct observation. In this study, the electronic structure and electrostatic effect of oxygen impurities at the MgO/Ag interface were investigated using ab-initio modeling. The oxygen impurities considered were interstitial (O_i), substitutional (O_{Ag}), and reconstructed substitutional (O_h) oxygen defects on the Ag-side interface layer.

2. Calculation details

First-principle calculations were performed based on the Kohn–Sham equation as implemented in the Vienna ab-initio simulation package code (VASP) [20]. The projector augmented wave (PAW) method [21] was used for describing ionic potentials, and the exchange-correlation function between the electrons were adopted for the Perdew, Burke, and Ernzerhof (PBE) potential [22]. The basis set of the plane waves was expanded to a cut-off energy of 400 eV and Gaussian smearing was used with a 0.1 eV of sigma value.

The (2×2) periodicity of supercells was constructed to describe the MgO film and Ag substrate. The supercell consisted of 2 layers of MgO and 4 layers of Ag wherein at the bottom the two layers were fixed at the bulk position. A vacuum thickness of 22 Å was set and the dipole correction was applied in all calculations. In a defect-free structure, substrate layers consisted of 8 Ag atoms and film layers contained 8 Mg and

* Corresponding author. Tel.: +82 2 2220 0507; fax: +82 2 2281 5308.

E-mail address: yongchae@hanyang.ac.kr (Y.-C. Chung).

8 O atoms. The oxygen impurities were generated on the Ag-side interface layer. The O_{Ag} was generated by substituting O atom with fourth layer of Ag atom. The O_i and O_h were generated by positioning oxygen on the hollow site of the face centered cubic (FCC) Ag (001). The difference between O_i and O_h is that O_h is a reconstructed substitutional oxygen defect which has a neighboring vacancy of the Ag site. The constituent atoms in MgO/Ag systems were fully relaxed until the maximum Hellmann–Feynman forces were in the range of 0.1 eV/Å. A Brillouin-zone integration scheme was used on a grid of $(2 \times 2 \times 1)$ Monkhorst–Pack points for ionic relaxation [23]. Then, $(6 \times 6 \times 1)$ k-point sampling scheme was employed for an accurate electronic structure. From the electronic structure, the electrostatic potential is the sum of the Hartree potential and the ionic potential. The xy plane averaged electrostatic potential was obtained using

$$\bar{V}(z) = \iint_A V(x, y, z) dx dy. \quad (1)$$

The work function of the system is defined as the electrostatic energy of vacuum level with respect to the Fermi energy.

$$\phi = V_{vac} - E_F \quad (2)$$

3. Results and discussion

3.1. Structural features

The O_i , O_{Ag} , and O_h have different interfacial distances and neighboring ions as shown in Fig. 1. The O_i is positioned on the hollow site of Ag (001) and the neighboring ion in the film is Mg cation. This position of oxygen induces the increase of interfacial distance by 0.06 Å. The interface distance is defined as the averaged distance between Ag and MgO atoms at the interface. The O_{Ag} is on the substitutional site of vacant site of interfacial Ag which has neighboring oxygen ion in the MgO film and is surrounded by Ag atoms in the interface and subinterface layers. Because of the repulsive force from neighboring oxygen ion, the O_{Ag} moves down to the subinterface layer. If the O_{Ag} overcome the repulsive force from oxygen ions in the film, a reconstructed structure, O_h , is generated. After the reconstruction, the oxygen impurity migrates to the hollow site of FCC Ag (001) neighboring Mg ion in the film. However, in the case of O_h , the interfacial distance did not increase because

the oxygen impurity can partially occupy the neighboring vacant site. All types of oxygen impurities at the MgO/Ag interface were positioned on the Ag side layer interface but they show different structural features.

3.2. Density of states

To understand the additional bonding between oxygen impurities and their neighboring ions, their density of state (DOS) is analyzed as shown in Fig. 2. For the case of defect-free MgO/Ag, oxygen atoms in the film have ionic bonding with Mg and weak covalent bonding with Ag [24]. When the oxygen impurity is generated, the states of oxygen atom in the film showed a similar DOS with that of defect-free MgO. On the other hand, the DOS of the interfacial oxygen impurities showed a significant change due to their neighboring ions [25]. The states of O_i and O_h were hybridized with the states of the interfacial Ag atoms and the O_{Ag} was hybridized with that of subinterface Ag atoms. The reason why O_{Ag} interacts with the subinterface Ag is that the subinterface Ag atom is the nearest neighbor due to the sinking of the O_{Ag} from the interfacial Ag layer. Thus, all types of oxygen impurities are associated with the Ag substrate. On the other hand, the interaction with the film is not for all types of oxygen impurity. The states of O_i show hybridization with the MgO film around the –5 eV. However, for the case of O_{Ag} and O_h , there was no significant hybridization between the oxygen impurities and MgO film as shown in Fig. 2(b) and (c). The DOS analysis indicates that all types of interfacial oxygen impurities were associated with Ag substrate but only O_i directly interacts with the MgO film.

3.3. Work function

When oxygen impurities are generated at the MgO/Ag interface, the electronic structure of the interface is modified and the work function of the interface is also changed. The altered work function is summarized in Table 1. When the work function of the clean Ag substrate is the reference, the changed work function can be expressed as below.

$$\Delta\phi = \phi - \phi_{Ag}. \quad (3)$$

According to our calculation, the work function of Ag was 4.18 eV (experimental value is 4.22 eV [27]). The work function decreased by 1.19 eV in defect-free MgO/Ag structure. In the interfacial oxygen impurity-containing structure, the work function is further changed compared with the defect-free structure. The O_i and O_h induced an

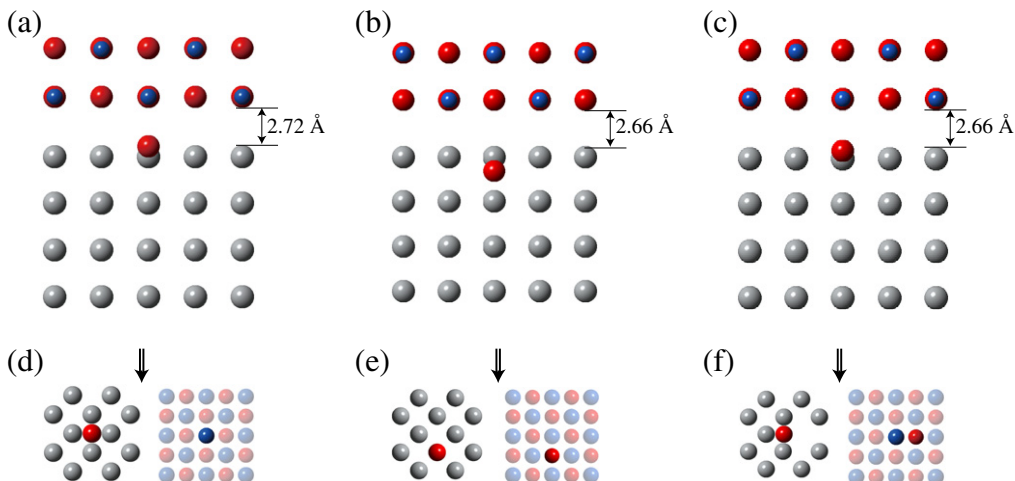


Fig. 1. Side cut view and top view of (a) O_i , (b) O_{Ag} , and (c) O_h -containing MgO/Ag structure. Note that the interfacial distance of O_i is longer than others. Top view of the substrate side interface layer (left) and film side interface layer (right) of (d) O_i , (e) O_{Ag} , and (f) O_h -containing MgO/Ag structure. The arrows in (d, e, f) are the perspective of the side cut view of (a, b, c), respectively. The highlighted atoms of the film side interface layer are neighboring ions with oxygen impurities or vacant site. The gray, red, and blue spheres represent the Ag, O, and Mg atoms, respectively.

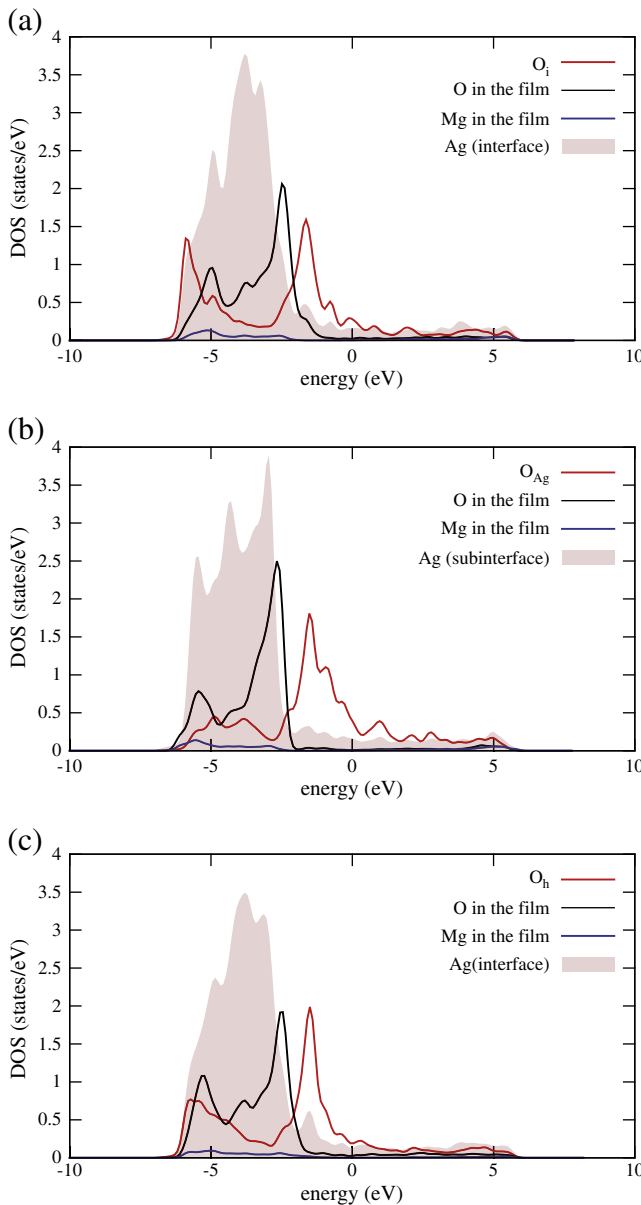


Fig. 2. Density of states of (a) O_i , (b) O_{Ag} , (c) O_h , and their neighboring Ag atom in substrates and neighboring O and Mg ions in the films. All of the oxygen impurities are associated with the Ag substrate but only O_i directly has a hybridized state with the film.

additional increase of the interface work function and O_{Ag} induces a slight decrease of the interface work function. The relative planar-averaged electrostatic potential in Fig. 3 obviously shows the work function change. The relative potential in a vacuum on the left side represents the work function of the substrate. The potential on the

Table 1

Structural and electronic properties of the defect-free, O_i , O_{Ag} , and O_h -containing MgO/Ag (100).

Structure	$d_{interface}$ (Å)	$q(O_{impurity})$ (e)	ϕ (eV)	$\Delta\phi$ (eV)
MgO/Ag	2.66	–	2.86	–1.32
MgO/ O_i -Ag	2.72	7.14	3.27	–0.91
MgO/ O_{Ag} -Ag	2.66	6.9	2.81	–1.37
MgO/ O_h -Ag	2.66	7.08	3.14	–1.04

Note: The $d_{interface}$ is the distance between the interface. The $q(O_{impurity})$ is the calculated Bader charge of the oxygen defect. The ϕ is the calculated work function and $\Delta\phi$ is the work function change with respect to the Ag (001) surface.

right side is associated with the modified work function induced by the interaction between the oxygen impurity and the MgO film.

3.4. Interface effect

The origin of $\Delta\phi$ is the potential level pinning induced by a surface dipole which is generated by the interface defect and film. According to the Helmholtz equation, the relation between the work function and the dipole can be expressed as [26]:

$$\Delta\phi = \frac{e\mu\cos\theta}{\epsilon_0 A} = -180.95 \frac{\mu_z}{A} \quad (4)$$

where ϵ_0 is the permittivity of the vacuum level, A is surface area, and μ is surface dipole moment directed along the surface normal (eÅ). Since the work function is determined by the relative vacuum level potential, the μ_z is the only component that affects the work function. The μ_z can be expressed as the sum of the dipole moment of the substrate (μ_s) that is the dipole of the oxygen impurity-containing the Ag substrate in the absence of the MgO film and the dipole moment created through the charge-redistribution that accompanies film deposition (μ_d), according to

$$\Delta\phi = -180.95 \frac{\mu_s + \mu_d}{A}. \quad (5)$$

By using the Helmholtz principle, the μ_s can be computed from the asymptotic vacuum level of each substrate as

$$\Delta V_{substrate} = V_{right} - V_{left} = \frac{e\mu_s}{\epsilon_0 A} \quad (6)$$

where V_{right} and V_{left} are the planar-averaged electrostatic potentials of the vacuum level on the impurity-contained surface side and clean substrate side. Table 2 summarizes the calculated μ_s , μ_d , and μ_z values.

From the calculated results, it can be seen that the surface dipole moment can be generated where the dipole moment of the substrate is zero. In the defect-free structure, such a dipole moment is generated only by the contribution of μ_d . The origin of the μ_d can be understood with the two contributions. One is charge redistribution due to the formation of interface bonding between the film and substrate. The other is the “compression effect” that pushes back the electrons which are spilled out from the metal surface where the dielectric layer is deposited. The compression effect is sensitive to the interfacial distance and generates larger surface dipole moment than interface bonding in the MgO/Ag system [10]. In the defect-free MgO/Ag structure, the work function change is induced by μ_d .

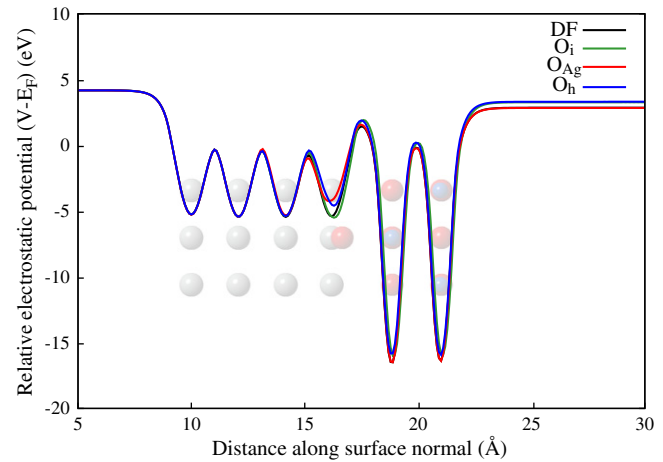


Fig. 3. Relative planar-averaged electrostatic potential for interface defective MgO/Ag systems as a function of position in the direction perpendicular to the surface.

Table 2

Vacuum level potential difference and related dipole moment of the defect-free, O_i , O_{Ag} , and O_h -containing MgO/Ag (100) system.

Structure	$\Delta V_{substrate}$ (eV)	μ_s/A (me/Å)	μ_d/A (me/Å)	μ_z/A (me/Å)	$\Delta\phi$ (eV)
MgO/Ag	0	0	6.58	6.58	−1.32
MgO/ O_i -Ag	0.202	−1.12	5.43	4.31	−0.91
MgO/ O_{Ag} -Ag	0	0	6.47	6.47	−1.37
MgO/ O_h -Ag	0.294	−1.62	6.65	5.03	−1.04

Note: $\Delta V_{substrate}$ is the difference in the asymptotic vacuum level potential of the substrate. The μ_s/A , μ_d/A , and μ_z/A are calculated substrate induced dipole, deposition induced dipole, and surface dipole, respectively. $\Delta\phi$ is the work function change with respect to the Ag (001) surface.

The induced μ_d in the defect-free MgO/Ag still remains where O_{Ag} and O_h are generated. For the case of O_{Ag} -contained MgO/Ag, μ_s is completely screened because of the sinking of O_{Ag} and the surface reconstruction. Relative to the defect-free MgO/Ag, the μ_d of O_{Ag} -contained MgO/Ag slightly decreased and $\Delta\phi$ decreased by 0.05 eV. On the other hand, O_h and its neighboring vacancy induce μ_s of −1.62 me/Å. The μ_s induced by O_h still remained after the deposition and contributed to the work function change. The μ_d was increased by 0.07 me/Å relative to the defect-free MgO/Ag. For the case of O_{Ag} and O_h , the μ_d remained similar to that of the defect-free structure.

On the other hand, O_i not only created μ_s but also induced changes of μ_d , relative to the defect-free structure. It can be inferred that the origin of the μ_d change is its increased interfacial distance and the interface bonding between O_i and MgO. Since the compression effect is sensitive to the interfacial distance, surface dipoles were induced by electron redistribution changes. Also, as shown in the DOS analysis, the formed interface bonding between O_i and MgO generated a surface dipole moment. Thus, O_i -containing MgO/Ag shows different μ_d with that of the defect-free structure.

4. Conclusion

In conclusion, the electrostatic effects of the three types of oxygen defects at the MgO/Ag (001) interface were investigated. The origin of the work function change was analyzed with a dipole contribution decoupled into the substrate and interface electron terms. Each term of the dipole moment has been associated with their structural features and interface bonding properties. The results of this study indicate that the type of oxygen impurities induces a significant effect on the electronic structure and work function of the interface.

The change of the work function indicates that the interface work function could be tunable by controlling the interfacial oxygen impurities. This work provides an important clue to designing ultra-thin oxide films on metal by controlling oxygen defects.

Acknowledgments

This work was supported by the National Research Foundation (NRF) grant funded by the Korean government (MEST) (No. 2012-0016945), the project of Global PhD Fellowship conducted by the National Research Foundation (NRF) in 2011, and the Basic Science Research Program through the National Research Foundation of Korea (NRF) funded by the Ministry of Education, Science and Technology (No. 2012-0026175).

References

- [1] L. Giordano, G. Pacchioni, Acc. Chem. Res. 44 (2011) 1244.
- [2] S. Altieri, L.H. Tjeng, G.A. Sawatzky, Thin Solid Films 400 (2001) 9.
- [3] J. Wollschläger, D. Erdös, H. Goldbach, R. Hpken, K.M. Schröder, Thin Solid Films 400 (2001) 1.
- [4] P. Giese, H. Kirsch, M. Wolf, C. Frischkorn, J. Phys. Chem. C 115 (2011) 10012.
- [5] K. Honkala, A. Hellman, H. Gröbeck, J. Phys. Chem. C 114 (2010) 7070.
- [6] L. Giordano, G. Pacchioni, Phys. Chem. Chem. Phys. 8 (2006) 3335.
- [7] H.-J. Shin, J. Jung, K. Motobayashi, S. Yanagisawa, Y. Morikawa, Y. Kim, M. Kawai, Nat. Mater. 9 (2010) 442.
- [8] T. Jaouen, G. Jézéquel, G. Delhaye, B. Lépine, P. Turban, P. Scheieffer, Appl. Phys. Lett. 97 (2010) 232104.
- [9] L. Giordano, F. Cinquini, G. Pacchioni, Phys. Rev. B 73 (2005) 045414.
- [10] S. Prada, U. Martínez, G. Pacchioni, Phys. Rev. B 78 (2008) 235423.
- [11] M. Bieletzki, T. Hyyninen, T.M. Soini, M. Pivetta, C.R. Henry, A.S. Foster, F. Esch, C. Barth, U. Heiz, Phys. Chem. Chem. Phys. 12 (2010) 3203.
- [12] T. Kol’nig, G.H. Simon, H.-P. Rust, M. Heyde, J. Phys. Chem. C 113 (2009) 11301.
- [13] J. Jung, H.-J. Shin, Y. Kim, M. Kawai, J. Am. Chem. Soc. 133 (2011) 6142.
- [14] O. Robach, G. Renaud, A. Barbier, Phys. Rev. B 60 (1999) 5858.
- [15] S. Rusponi, C. Boragno, U. Valbusa, Phys. Rev. Lett. 78 (1997) 2795.
- [16] G. Renaud, P. Guénard, A. Barbier, Phys. Rev. B 58 (1998) 7310.
- [17] C. Noguera, J. Godet, J. Goniakowski, Phys. Rev. B 81 (2010) 155409.
- [18] M. Rocca, L. Savio, L. Vattuone, U. Burghaus, V. Palomba, N. Novelli, Phys. Rev. B 61 (2000) 213.
- [19] L. Vattuone, U. Burghaus, L. Savio, M. Rocca, G. Costantini, F. de Mongeot, C. Boragno, S. Rusponi, U. Valbusa, J. Chem. Phys. 115 (2001) 3346.
- [20] G. Kresse, J. Furthmüller, Comput. Mater. Sci. 6 (1996) 15.
- [21] J.P. Perdew, J.A. Chevary, S.H. Vosko, K.A. Jackson, M.R. Pederson, D.J. Singh, C. Fiolhais, Phys. Rev. B 94 (2005) 175501.
- [22] J.P. Perdew, K. Burke, M. Ernzerhof, Phys. Rev. Lett. 77 (1996) 3865.
- [23] H.J. Monkhorst, J.D. Pack, Phys. Rev. B 13 (1976) 5188.
- [24] N. Lopez, S. Valeri, Phys. Rev. B 70 (2004) 125428.
- [25] J.P. Allen, D.O. Scanlon, G.W. Watson, Phys. Rev. B 84 (2011) 115141.
- [26] A.Y. Anagaw, R.A. Wolkow, G.A. DiLabio, J. Phys. Chem. C 112 (2008) 3780.
- [27] M. Chelvayohan, C.H.B. Mee, J. Phys. C 15 (1982) 2308.